

## Behavior of Polycatalytic Assemblies in a Substrate-Displaying Matrix

Renjun Pei,<sup>‡</sup> Steven K. Taylor,<sup>‡</sup> Darko Stefanovic,<sup>§</sup> Sergei Rudchenko,<sup>†</sup>  
Tiffany E. Mitchell,<sup>‡</sup> and Milan N. Stojanovic\*<sup>‡</sup>

*Contribution from the NSF Chemical Bonding Center: Center for Molecular Cybernetics, Division of Experimental Therapeutics, Department of Medicine, Columbia University, New York, New York 10032, Department of Computer Science, University of New Mexico, Albuquerque, New Mexico 87131, and Hospital for Special Surgery, New York, New York 10021*

Received December 11, 2005; E-mail: mns18@columbia.edu

**Abstract:** We describe polycatalytic assemblies, comprising one or two streptavidin molecules and two to six attached nucleic acid catalysts (deoxyribozymes), with phosphodiesterase activity. When exposed to a matrix covered at high densities with oligonucleotide substrates, these molecules diffuse through the matrix continuously cleaving the substrate at rates comparable to those of individual catalysts in solution. Rates of diffusion (movement), processivity, and resident times of assemblies can be controlled through the number of catalytic units and the length of substrate/product recognition regions. The assemblies were characterized at the ensemble level using surface plasmon resonance.

### Introduction

Within the context of our project on molecular devices<sup>1–15</sup> with in vivo therapeutic applications,<sup>1,2</sup> we were interested in molecules that could diffuse through a matrix and release a product, while not leaving the matrix. Because we were interested in controlling the rate of diffusion of the molecules using molecular-scale computation elements,<sup>1,2</sup> we focused on constructing such molecular assemblies from nucleic acid catalysts.

While studying the movement of various polypeds, in particular spiders,<sup>16</sup> it occurred to us that we could achieve the desired behavior through a combination of multipedal design

and catalytic activity of nucleic acids: polycatalytic assemblies could use a multivalent (or multipedal<sup>17,18</sup>) variation of the random walk<sup>19</sup> to cleave their oligonucleotide substrates displayed on various matrices (Figure 1a). We also hypothesized that such assemblies would preferably move to the areas covered with new substrates, i.e., they would undergo biased diffusion,<sup>20,21</sup> like other enzymes moving through substrate matrices.<sup>22–23</sup>

The deoxyribozymes **8–17** (with phosphodiesterase or cleavage activity, Figure 1b<sup>24,25</sup>) bind to their substrates (and products) through Watson–Crick base pair formation, forming an active enzyme–substrate complex, which results in the cleavage of a phosphodiester bond and, finally, in the release of products. If we couple (Figure 1a) four deoxyribozymes to streptavidin and expose a matrix covered with substrates to this construct, cumulative binding of multiple catalysts to substrates will bind the assembly tightly to the matrix, whereas individual catalysts will still be able to rapidly cleave substrates, release products,

<sup>‡</sup> Columbia University.

<sup>§</sup> University of New Mexico.

<sup>†</sup> Hospital for Special Surgery.

- (1) (a) Stojanovic, M. N.; Mitchell, T. E.; Stefanovic, D. *J. Am. Chem. Soc.* **2002**, *124*, 3555–61. (b) Stojanovic, M. N.; Stefanovic, D. *Nat. Biotechnol.* **2003**, *21*, 1069–74.
- (2) Kolpashchikov, M.; Stojanovic, M. *J. Am. Chem. Soc.* **2005**, *127*, 11348–11351.
- (3) (a) Badjic, J. D.; Bazani, C.; Credi, A.; Silvi, S.; Stoddart, J. F. *Science* **2004**, *303*, 1845–9. (b) Shirai, Y.; Osgood, A. J.; Zhao, Y.; Kelly, K. F.; Tour, J. M. *Nano Lett.* **2005**, *5*, 2330–4.
- (4) Sestelo, J. P.; Kelly, T. R. *Appl. Phys. A* **2002**, *75*, 337–43.
- (5) Feringa, B. L.; van Delden, R. A.; Wiel, M. K. *J. Pure Appl. Chem.* **2002**, *75*, 563–75.
- (6) Hernández, J. V.; Kay, E. R.; Leigh, D. A. *Science* **2004**, *306*, 1532–7.
- (7) Yurke, B.; Turberfield, A.; Mills, A. P., Jr.; Simmel, F.; Neumann, J. *Nature* **2000**, *406*, 605–8.
- (8) Yurke, B.; Turberfield, A.; Mills, A. P., Jr.; Simmel, F.; Neumann, J. *Phys. Rev. Lett.* **2003**, *90*, 118102–3.
- (9) Yan, H.; Zhang, X.; Shen, Z.; Seeman, N. C. *Nature* **2002**, *415*, 62–65.
- (10) Chen, Y.; Wang, M.; Mao, C. *Angew. Chem., Int. Ed.* **2004**, *43*, 3554–7.
- (11) Sherman, W. B.; Seeman, N. C. *Nano Lett.* **2004**, *4*, 1203–7.
- (12) Shin, J. S.; Pierce, N. A. *J. Am. Chem. Soc.* **2004**, *126*, 10834–5.
- (13) Yin, P.; Yan, H.; Daniell, X. G.; Turberfield, A. J.; Reif, J. H. *Angew. Chem., Int. Ed.* **2004**, *43*, 4906–11.
- (14) Tian, Y.; He, Y.; Chen, Y.; Yin, P.; Mao, C. *Angew. Chem., Int. Ed.* **2005**, *44*, 4355–8.
- (15) Bath, J.; Green, S. J.; Turberfield, A. *J. Am. Chem. Soc.* **2005**, *127*, 4358–61.

- (16) (a) Fichter, E. F.; Fichter, B. L. A survey of legs of insects and spiders from a kinematic perspective. In *IEEE International Conference on Robotics and Automation*; 1988; Vol. 2, pp 984–86. (b) Full, R. J. Biological inspiration: Lessons from many-legged locomotors. In *Robotics Research Ninth International Symposium*, 2000; Hollerbach, J., Koditschek, D., Eds.; Springer-Verlag: London, pp 337–41.
- (17) Mammen, M.; Whitesides, G. *Angew. Chem., Int. Ed.* **1998**, *37*, 2754–94.
- (18) Choi, S.-K. *Synthetic Multivalent Molecules: Concepts and Biomedical Applications*; John Wiley and Sons, Inc.: New York, 2004.
- (19) Berg, H. C. *Random Walks in Biology*; Princeton University Press: Princeton, NJ, 1993.
- (20) Antal, T.; Krapivsky, P. L. *Phys. Rev. E* **2005**, *72*, 046104–1–12.
- (21) Saffarian, S.; Collier, I. E.; Marmer, B. L.; Elson, E. L.; Goldberg, G. *Science* **2004**, *306*, 108–11.
- (22) Triguante, G.; Gast, A. P.; Robertson, C. R. *J. Colloid Interface Sci.* **1999**, *213*, 81–6.
- (23) Hyun, J.; Kim, J.; Craig, S. L.; Chilkoti, A. *J. Am. Chem. Soc.* **2004**, *126*, 4770–1.
- (24) Emilsson, G. M.; Breaker, R. R. *Cell. Mol. Life Sci.* **2002**, *59*, 596–607.
- (25) Santoro, S. W.; Joyce, G. F. *Proc. Nat. Acad. Sci. U.S.A.* **1997**, *94*, 4262–6.

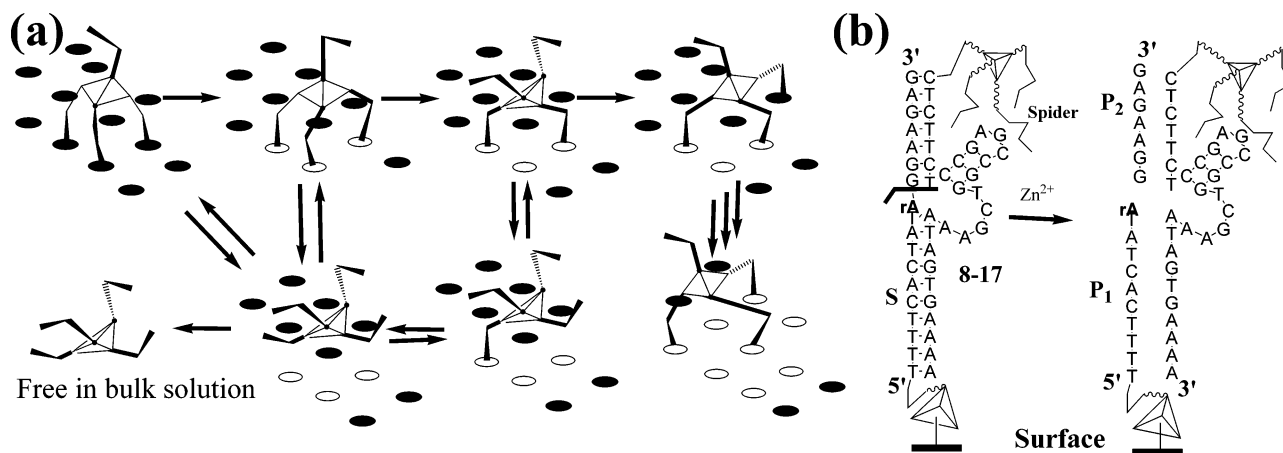


**Figure 1.** (a) Proposed diffusion of a single polycatalytic assembly in a matrix covered with substrates (projection depicted): the assembly attaches itself to the matrix with multivalent binding to substrates (filled ellipses). Turnover of substrates to products (hollow ellipses) is followed by dissociation and rebinding to new substrates, leading to the diffusion coupled with the cleavage of substrates in the matrix. (b) The elementary reaction of assemblies cleaving substrates deposited on recognition landscapes: the catalytic unit is based on the deoxyribozyme 8–17 cleaving substrate (S) and releasing products (P<sub>1</sub> and P<sub>2</sub>).

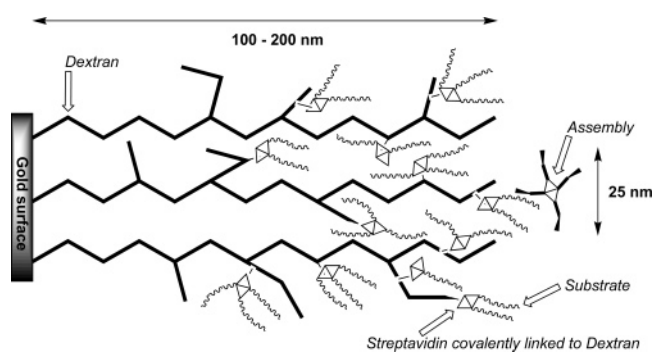


**Figure 2.** Schematic representation of a hydrogel matrix (three dextran oligomers shown). The hydrogel has a depth of 100–200 nm. The assemblies with four catalytic units have an estimated diameter of 25 nm. The individual dextran chains, substrates, and catalysts are flexible, improving the access to new substrates. Note that substrates are not equally distributed throughout the matrix.

and bind new substrates<sup>26,27</sup> through the process of dissociation and rebinding.

In this work, we study polycatalytic assemblies with 2–6 catalytic units based on 8–17 in a three-dimensional dextran–streptavidin matrix (a hydrogel made of dextran oligomers, as depicted in Figure 2) displaying oligonucleotide substrates at high concentrations. We use surface plasmon resonance (SPR) to follow the release of products from the matrix<sup>28</sup> and to determine the rate of cleavage and the processivity of the polycatalytic assemblies.

## Results and Discussion

**Synthesis of Polycatalytic Assemblies.** We assembled and purified 11 different polycatalytic assemblies (Figure 3) using a modified method reported previously.<sup>29</sup> Individual species were named NICK-*X*.NA, where *X* denotes the number of catalysts (or “legs”, in this work *X* = 2, 3, 4, or 6) and *N* denotes the number of A’s in the P<sub>1</sub> recognition region (in this work, *N*

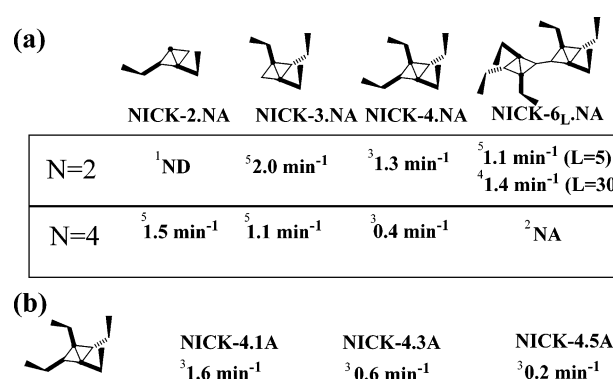


**Figure 3.** (a) Rates of cleavage in the matrix for various assemblies with an increasing number of catalytic units. (b) Assemblies that were studied only with four catalytic units. <sup>1</sup>Not determined, fast dissociation precluded precise determination of rates. <sup>2</sup>Not synthesized. <sup>3</sup>Determined during minutes 5–9 (<20% of cleavage) of sensorgrams shown in Figure 7b. <sup>4</sup>The average from two sensorgrams, during minutes 5–9, one of which is given in Figure 7a. <sup>5</sup>Determined during minutes 5–9 (<20% of cleavage) of sensorgrams shown in the Supporting Information (Figure S10).

= 1–5; for example, 4 in Figure 1b). NICK is an acronym for Nanoassembly Incorporating Catalytic Kinesis because they couple diffusion (movement) to a catalytic process. For example, NICK-4.4A is a species with 4 catalytic units, each with 4 A’s in the 3’ (or P<sub>1</sub>) recognition region. Assemblies with two streptavidins and six catalytic units NICK-6<sub>5</sub>.2A and NICK-6<sub>30</sub>.2A have their streptavidins linked via oligonucleotides with 5 and 30 T’s, respectively, and biotins at both 5’ and 3’ ends.

After synthesis, assemblies were tested for their ability to diffuse through the matrix while cleaving substrates. Substrates were displayed at concentrations of about 3 mM (assuming a 100 nm layer depth) and estimated intersubstrate distances of approximately 9 nm. The ethylene glycol based spacers used to attach substrates to the streptavidin in the matrix and catalysts to streptavidin are very flexible; these properties allow the catalytic units to capture a new substrate very efficiently.

The progression of a typical experiment using SPR is shown in Figure 4. A drop in response units (RU) in a channel containing both assemblies and substrates is used to calculate the number of cleaved substrates per assembly and to follow the diffusion of the assembly in the matrix in real time.

(26) Nieba, L.; Krebber, A.; Plückthun, A. *Anal. Biochem.* **1996**, *234*, 155–65.

(27) Lieto, A. M.; Lagerholm, B. C.; Thompson, N. L. *Langmuir* **2003**, *19*, 1782–87.

(28) Nyholm, T.; Andang, M.; Bandholtz, A.; Maijgren, C.; Persson, B.; Hotchkiss, G.; Fehniger, T. E.; Larsson, S.; Ahrlund-Richter, L. *J. Biochem. Biophys. Methods* **2000**, *44*, 41–57.

(29) Park, S.-J.; Lazarides, A. A.; Mirkin, C. A.; Letsinger, R. L. *Angew. Chem.* **2001**, *113*, 2993–6.

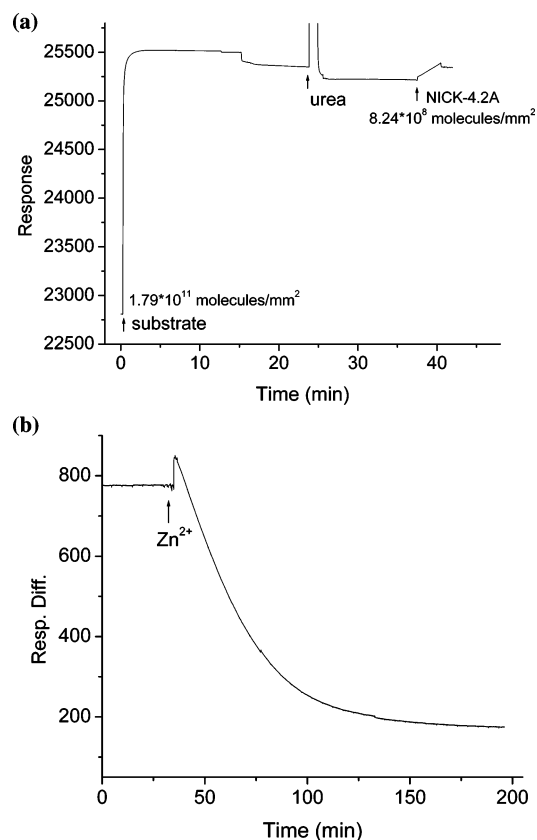


**Figure 4.** Typical sensorgrams: (a) Time course of substrate and NICK-4.2A deposition (response (in response units) vs time (min); response in channel 2 with assemblies attached is shown). First, a substrate is attached (in HBS-EP buffer), resulting in an increase in mass. Next, a nonspecifically bound substrate is desorbed by urea (leaving the substrate at  $\Delta = 2411.1$  RU or  $2.4111$  ng  $\text{mm}^{-2}$  or  $1.79 \times 10^{11}$  molecules  $\text{mm}^{-2}$ ); then NICK-4.2A's are attached ( $\Delta = 129.7$  RU or  $0.1297$  ng  $\text{mm}^{-2}$  or  $8.24 \times 10^8$  molecules  $\text{mm}^{-2}$ , in HBS-EP buffer). Response units (RU) can be converted to mass using the standard formula  $1000$  RU =  $1$  ng  $\text{mm}^{-2}$ . (b) Time course of product formation and release (the difference between two channels, with and without assemblies (RU(channel 2) – RU(channel 1)), is shown). Cleavage is initiated by the addition of a metal ion (switch to HBS-Zn buffer) and is visualized by a release of the product and a decrease in mass on the chip. The control channel is coated with substrates only.

**Behavior of NICK-4.2A in the Matrix.** Our initial experiments were performed on an assembly with 4 catalytic units and 2 A's in the  $P_1$  recognition region (NICK-4.2A). Figure 5a illustrates that in the absence of flow and at very high ratios of substrates to assemblies (3800:1) the nearly linear increase in the number of cleaved substrates continues for over 70% of the reaction time course (over 2700 turnovers per assembly or over 675 turnovers per catalyst). The observed cleavage rate per assembly in this period was  $5.5$   $\text{min}^{-1}$  (or  $1.3$   $\text{min}^{-1}$  per catalyst).

The maximal leg span of the tetracatalytic assembly can be estimated to be 20–25 nm. Assuming a 100 nm depth of the dextran layer, we can estimate that the volume covered by each NICK-4.2A upon cleavage of 3500 substrates is defined by a cube with sides measuring 100 nm or at least 64 times larger than the volume an assembly might be able to reach in theory without diffusion. However, precise calculation of distances covered by assemblies and visualization of paths would require the application of single molecule techniques, and this is beyond the scope of the current manuscript.

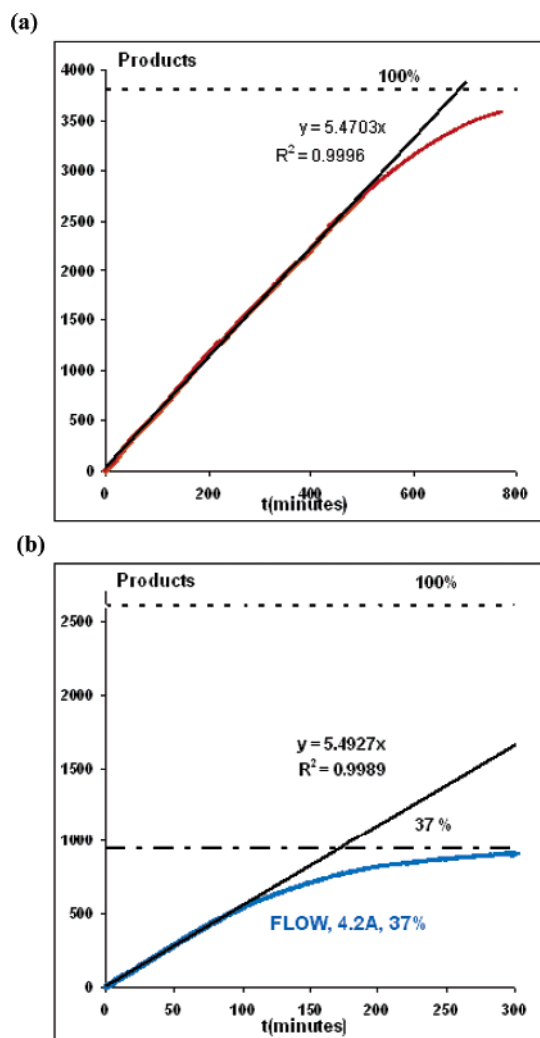


**Figure 5.** (a) Sensorgram for the no-flow experiment, NICK-4.2A, at high dilutions (1:3800); the assembly cleaves 100% of the substrate offered and shows a time-linear increase in the amount of released product (the black line is a trend line through the first 2500 cleavage events). (b) NICK-4.2A under flow conditions ( $20$   $\mu\text{L min}^{-1}$ ) has low processivity (37%) under high dilution with substrates (1:2600, the black line is a trend line over the first 500 turnovers).

The persistence of a constant rate of cleavage over prolonged periods of diffusion, despite traditionally strong product inhibition displayed by deoxyribozymes, argues that assemblies are in a similar environment, that is, surrounded by the similar concentrations of substrates for a prolonged period of time, despite cleavage. This result is consistent with the proposal in Figure 1a, and it eliminates an alternative mechanism of diffusion, in which an assembly would trap itself in a perimeter of cleaved substrates without any movement of its center of mass and then complete dissociation of all catalysts would be required for further cleavage (and hence diffusion). The similarity between the solution-phase rate of cleavage and the rate of cleavage within a matrix also argues against an alternative mechanism in which an assembly would cleave only substrates it bound initially and would have to dissociate all its catalytic units before diffusing to another position. Thus, although the precise details of the mechanism of diffusion can be ascertained only with further studies on single molecules, the totality of experiments suggests that the assemblies continuously diffuse through the matrix with individual catalytic units randomly

dissociating and rebinding to either products or substrates, as shown in Figure 1a.

**Influence of Flow.** Flow of buffer in the SPR channel does not change the initial rates of cleavage (cf. Figures 5a and 5b; both rates are  $5.5 \text{ min}^{-1}$  per **NICK-4.2A** or  $\sim 1.3 \text{ min}^{-1}$  per leg), but it limits the maximum average turnover per substrate at higher substrate to assembly ratios. For example, with a flow of  $20 \mu\text{L min}^{-1}$ , **NICK-4.2A** has nearly the same rate for the first 500 cleavages as in the experiment without flow but is unable, on average, to cleave more than 950 substrates (even out of the 2600 available; thus, the assembly has a cleavage efficacy of 37%). Further, in this experiment, no substantial cleavage activity can be detected with this assembly after 300 min. This is consistent with the suggestion that, on average for every 950 substrates cleaved, assemblies partitioned once into the bulk solution, where they are carried away by the flow (cf. Figure 1a).

In Figure 6a, we compare dissociation phases of sensorgrams in which **NICK-4.2A** was applied to substrate- and product-covered matrices. From these dissociation curves, we can conclude that each assembly partitions to the bulk solution from the product surface once every 100 min (at approximately 1:450 ratios to products), whereas during the same 100 min the dissociation from a substrate-covered surface is less than 20%. This suggests that for the first 500 cleavages, during which the cleavage rate is almost constant even in the presence of flow (linear portion of Figure 5b), the deoxyribozymes are binding new substrates at a rate similar to the rate at which individual catalytic units are dissociating; namely, assemblies do not behave to any appreciable extent as if they are bound to a product surface. In the second phase of the reaction (nonlinear phase in Figure 5b), assemblies behave as if they are increasingly bound to the product-covered areas and they partition at a steady rate in the bulk solution.

At low ratios of substrates to assemblies ( $\sim 240:1$ ), changing the flow rate influenced **NICK-4.2A** only minimally (Figure 6b), and cleavage progress remained nearly identical. This is consistent with the ability of assemblies to diffuse over the product-covered areas and, in no-flow experiments, with assemblies partitioning to the bulk solution at the later stages of the reaction having a high probability of rebinding back to the product-covered surface. Results with intermediate densities of assemblies in the matrix (1:850), which are provided in the Supporting Information, fit this model of behavior as well.

**Increasing the Processivity of Assemblies.** In the context of our experiments, the “processivity” can be defined as a number of catalytic cleavages taken without dissociation from the matrix. On the basis of the proposed mechanism (Figure 1a), we made a testable prediction that we can change processivity (that is, percent of cleaved substrate) by changing the  $k_{\text{off}}(\mathbf{P}_1)$  and  $k_{\text{on}}(\mathbf{P}_1)$  values of the catalytic units. We reasoned that the decrease in the  $k_{\text{off}}(\mathbf{P}_1)$  value may reduce the rate of cleavage of individual catalysts but will, even more so, decrease partitioning in the solution of the assemblies (because the rate of the multivalent diffusion will depend on the rate of the individual catalyst, whereas partitioning in the bulk solvent will depend on a cumulative dissociation constant). For example, the  $\mathbf{P}_1$  recognition regions of **2A** and **4A** catalysts have a  $k_{\text{off}}(\mathbf{P}_1)$  of  $\sim 22$  and  $8.4 \text{ min}^{-1}$ , respectively (Supporting Informa-

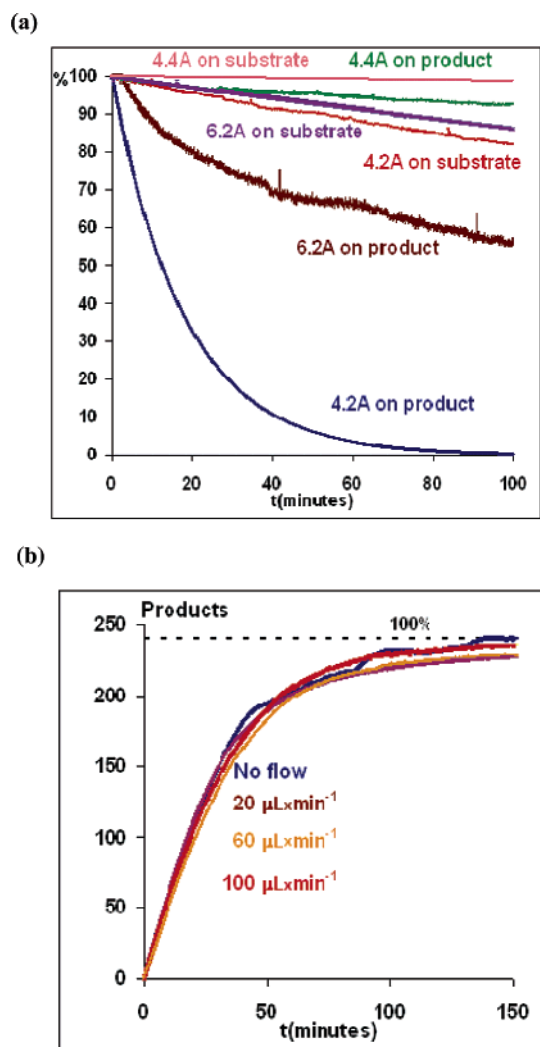


**Figure 6.** (a) Dissociation curves for the following. Red trace: **NICK-4.2A** on an uncleavable (substrate in which rA was substituted with A) substrate-covered matrix (1:460 ratio of assembly to substrate). Blue trace: **NICK-4.2A** on a  $\mathbf{P}_1$ -covered matrix (1:430 ratio of assembly to product). Coral trace: **NICK-4.4A** on an uncleavable substrate-covered matrix (1:520 ratio of assembly to substrate). Green trace: **NICK-4.4A** on a  $\mathbf{P}_1$ -covered matrix (1:540 ratio of assembly to product). Violet trace: **NICK-6<sub>15</sub>.2A** on an uncleavable substrate-covered matrix (1:1160 ratio of assembly to substrate). Brown trace: **NICK-6<sub>30</sub>.2A** on a  $\mathbf{P}_1$ -covered matrix (1:1132 ratio of assembly to product). (b) Sensorgrams of **NICK-4.2A** at a  $\sim 1:240$  ratio of assembly to substrates at the different flow rates.

tion), and **4A** deoxyribozymes have a higher  $k_{\text{on}}(\mathbf{P}_1)$  rate than **2A** deoxyribozymes. Thus, we would expect individual deoxyribozymes within **NICK-4.4A** to dissociate more slowly than those within **NICK-4.2A**, and once dissociated, they would also have a higher probability of rebinding to either substrates or products in the vicinity, before another deoxyribozyme dissociates. This should lead to an increase in processivity per Figure 1a, and we observed exactly this trend (Figure 7a).

As predicted, we observed a dramatic increase in substrate cleaving efficacy under flow conditions of **NICK-4.4A** vs

- (30) Piccolino, M. *Nat. Rev. Mol. Cell Biol.* **2000**, *1*, 149–53.  
 (31) (a) For a single motor: Okada, Y.; Hirokawa, N. *Science* **1999**, *283*, 1152–57. For multiple motors: (b) Diehl, M. R.; Zhang, K.; Lee, H. J.; Tirrell, D. A. *Science* **2006**, *311*, 1488–71. (c) Klumpp, S.; Lipowsky, R. *Proc. Natl. Acad. Sci.* **2005**, *102*, 17284–89 and literature cited therein.  
 (32) Niemeyer, C. M. *Rev. Mol. Biotechnol.* **2001**, *82*(1), 47–66.  
 (33) Niemeyer, C. M.; Adler, M.; Gao, S.; Chi, L. *Angew. Chem., Int. Ed.* **2000**, *39*(17), 3055–9.



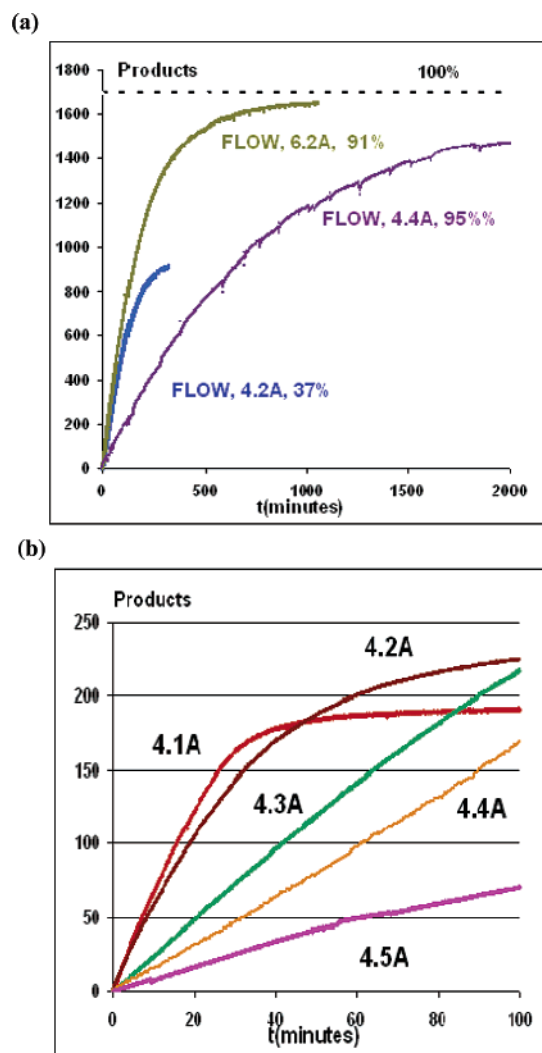


**Figure 7.** (a) Sensorgrams (y-axis is products released per assembly) of selected assemblies showing processivity under flow conditions ( $20 \mu\text{L min}^{-1}$ ). Blue trace: **NICK-4.2A** with low processivity (37%) under high dilution with substrates (1:2600), as in Figure 4B. Violet trace: **NICK-4.4A** with processivity over 95% at a 1:1670 ratio of assemblies to substrate (we are showing only the first 2000 out of 3600 min). Green trace: **NICK-6.2A** with grazing efficacy over 90% at a 1:1800 ratio with substrate. 100% line shown is for **NICK-4.4A**. (b) Cleavage of substrates for assemblies (at ratios  $\sim$  1:200 to 1:400) with a different number of A's in the substrate-recognition region under flow conditions ( $20 \mu\text{L min}^{-1}$ ).

**NICK-4.2A** at high dilutions of assemblies. In contrast to **NICK-4.2A** with 8 base pairs in the  $\text{P}_1$  recognition region, **NICK-4.4A** with 10 base pairs is able to cleave more than 95% of the substrates even at high ratios of substrates to assemblies (1670:1; Figure 7a, violet trace, only the first 2000 min are shown; the cleavage was followed for another 1500 min, but results are not shown for clarity). This is consistent with almost negligible dissociation of **NICK-4.4A** from both product- and substrate-covered matrices (i.e., a low probability of all four catalysts dissociating from the matrix at the same time cf. Figure 6a), while single catalysts continue to dissociate at respectable levels ( $\sim 8.4 \text{ min}^{-1}$ ; Supporting Information).

We observed the opposite trend when comparing **NICK 4.1A** (with only 7 base pairs in the  $\text{P}_1$  recognition region) with a first-order rate constant  $k_{\text{off}}(\text{P}_1)$  for this region of  $\sim 48 \text{ min}^{-1}$  to **NICK-4.2A**. Although the latter cleaves almost 96% of available substrates at 240:1 ratios to assemblies (Figure 7b, brown trace),

the former more rapidly dissociates from the surface (Supporting Information) and therefore does not cleave more than 65% of the substrates even at a 320:1 ratio (Figure 7b, red trace).

Another approach to reduce loss due to partitioning outside the matrix is to increase the number of catalytic units. Adding two more catalytic units in **NICK-6.2A** increased the number of visited substrate sites (Figure 7a, green trace) to at least 1650 out of  $\sim 1800$  available. There are important differences in these two approaches to increasing the processivity. Increasing the length of the hybridization arms always decreases the rate of cleavage and movement per assembly. In contrast, increasing the number of catalytic units from 4 to 6 does not decrease the overall rate of cleavage, and accordingly, it does not decrease the overall rate of diffusion.

**Rates vs Length of the  $\text{P}_1$  Recognition Region of Catalytic Units.** The rates of cleavage in the initial stages of experiments can be used as proxies for the rates of diffusion, if we assume that the mechanism in Figure 1a is correct. Thus, these rates would tell us how comparatively “agile” the individual assemblies are while diffusing through the matrix.

Accordingly, we compared the rates of five assemblies at higher ratios to substrates (1:200–1:400). (Rates of cleavage per assembly could be determined more precisely at such high ratios because of the larger error in determining amounts of assemblies at lower ratios.) These initial cleavage rates are not influenced significantly by the ratios to substrates; the specific time period (5–9 min, or below 20% of substrates cleaved) reported in Figures 3b and 3c was selected because it matched well for the **NICK-4.2A** rates observed in prolonged linear periods in Figures 5a and 5b. The rates include a small error in dissociation of assemblies from the surface being superimposed on substrate cleavage. However, this error is negligible for the ratios to substrates studied in these experiments in the short observation periods and, in particular, for assemblies with 4 and 6 catalytic units.

In Figure 7b, we show sensorgrams for five assemblies differing only in the length of the  $\text{P}_1$  recognition regions. The trends in observed rates of cleavage per leg (rate  $\times$  leg $^{-1}$  values: 1.6 for **1A**, 1.3 for **2A**, 0.6 for **3A**, 0.4 for **4A**, and 0.2  $\text{min}^{-1}$  for **5A**) suggest the importance of interactions with  $\text{P}_1$  for the rate of movement through the matrix. These values are also similar to the  $V_{\text{max}}$  values obtained in solution with fluorogenic substrates.

**Comment on the Behavior of Free, Single Deoxyribozymes in the Matrix.** Because the dissociation of the **2A** deoxyribozymes from the matrix displaying  $\text{P}_1$  is similar to that for the  $\text{P}_1$  binding region in the solution phase (Supporting Information), a single enzyme rapidly diffuses out of the matrix, without significant rebinding to products even at high concentrations of the product in the matrix. Using our standard procedure with cleavable substrates in both channels and an enzyme deposited in only one channel (in the EDTA-containing buffer, followed by switching to the  $\text{Zn}^{2+}$ -containing buffer), we were not successful in obtaining reliable estimates of the number of substrates cleaved by individual deoxyribozymes; the dissociation rate of a single enzyme from the matrix during the buffer switching procedure was too fast to determine reliably the initial amount of catalysts. For example, under these conditions, we estimated that the **4A** deoxyribozyme underwent less than one turnover.

To obtain even a rough estimate of the turnover, we had to apply modified conditions: one channel (control) was covered with an uncleavable substrate (with A substituted for rA), in an attempt to estimate the initial load of enzymes in the  $\text{Zn}^{2+}$ -containing buffer. This method allowed us to approximate that, at best, the average turnover for the **4A** deoxyribozyme was 3, whereas for the **2A** deoxyribozyme, the turnover was below 6. These results suggest that assemblies with single catalytic units are not capable of efficient and prolonged movement through the dextran–streptavidin matrix and that multivalency is necessary for processivity.

Our observation that single enzymes without streptavidin are completely removed from the matrix in a matter of minutes, if not seconds, while multicatalytic species bind very tightly is also consistent with the picture of individual catalysts within assemblies undergoing rapid dissociation and association, while the overall assembly remains bound to the matrix.

## Conclusions

In this work, we accomplished our initial goals, that is, the release of an oligonucleotide product ( $\text{P}_2$ ), with minimal removal of an assembly from the matrix (cf. **NICK-4A**) despite flow. Specifically, we report the following progress: (1) construction of polycatalytic assemblies, capable of continuously diffusing through a matrix via a process of biased diffusion; (2) demonstration of control over the rate of diffusion through variations in recognition regions and number of catalytic units; (3) minimization of loss due to diffusion outside of the matrix by increasing either the number of catalytic units per assembly or the number of bases in the substrate (or product) recognition regions. Our progress indicates that our design fulfills several key requirements needed for future studies involving drug release: (1) potential for linear increase in the released product over time; (2) autonomous diffusion through a matrix, without significant diffusion outside of the matrix; (3) controllable rate of diffusion.

Because our initial inspiration for this work was the behavior of spiders and the way they move in two dimensions, rapidly changing direction, quickly lifting and lowering their legs, and occasionally jumping, we propose to name these polycatalytic assemblies “spider molecules” or, simply, “spiders”. In our opinion, the proposed name gives the reader a good mental image of the behavior of the individual catalytic units (“spider legs”) attached to a streptavidin core (“body”) during the diffusion (movement) of polycatalytic assemblies (spiders) through the matrix.

Close analogues to spiders are diffusing enzymes, which dissociate, rebind, and cleave their substrates attached to 2D surfaces or to 3D matrices (e.g., collagenase or DNAses<sup>20–23</sup>). However, the overall behavior of **NICK-4A**, combining multivalent catalytic activity with the ability to diffuse (move) through the matrix and to destroy tracks made of substrates, seems unprecedented. Nevertheless, various aspects of the assemblies’ diffusion through the matrix resemble known processes. Natural motors<sup>30,31</sup> using tracks to bias diffusion, can be engineered to have more (or less) than two heads,<sup>31</sup> and walk in a stepwise fashion but do not degrade tracks. Artificial walkers that use tracks are fueled by the addition of fuel and “antifuel” molecules,<sup>3–14</sup> with the exception of a nicking enzyme-powered oligonucleotide.<sup>15</sup> Artificial motors based on

deoxyribozymes are currently limited to continuous conformational changes in solution,<sup>8,10</sup> although a crawling capability of deoxyribozymes with long substrate recognition regions has been proposed to occur over four positions.<sup>14</sup>

We will report on our progress in controlling the rate of diffusion of assemblies by molecular computation<sup>1,2</sup> shortly.

## Experimental

**Materials.** All oligonucleotides were custom-made and purified by Integrated DNA Technologies Inc. (Coralville, IA) or Trilink Biotechnologies Inc. (San Diego, CA) and used as received, except when noted. All SPR experiments were performed in 10 mM HEPES (pH = 7.4) with 0.15 M NaCl and DNA/RNase purified water (HBS buffer) at 25 °C. Loading of the assemblies was performed in HBS-EP buffer (HBS with 3 mM EDTA and 0.005% P20 surfactant). The cleavage reaction was performed in HBS-Zn buffer (HBS with 1 mM  $\text{ZnCl}_2$ ). Sequences of oligonucleotides were as follows.

Catalytic units (Spider “Legs”): 5′-Biotin-(TEG)-SP(18)-SP(18)-CTCTTCTCCGAGCC GGTCGAAATAGTG  $A_{(1-5)}$

Linkers: 5′-Biotin-(TEG)-T<sub>50r30</sub>-(TEG)-Biotin

Substrate: 5′-Biotin-SP(18)-SP(18)-TTTTTTTTTCACTATrAGG AA-GAG (where TEG is a tetraethylene glycol spacer, SP(18) is an 18-atom hexaethylene glycol spacer, and “r” precedes a ribonucleotide).

**Instrumental.** For SPR experiments, we used the Biacore X system and commercially available Biacore SA sensor chips from Biacore AB (Uppsala, Sweden). Solution-phase kinetic experiments are described in the Supporting Information. For HPLC purification we used a Shimadzu LC-6AD pump equipped with an SPD-M10A PDA detector. Exact conditions are provided in the Supporting Information. Absorbance ratios of 260/280 were determined on an Amersham Biosciences Ultrospec 3300 pro UV/visible spectrophotometer.

**Construction of Polycatalytic Assemblies.** Assemblies with 2, 3, and 4 catalytic units were assembled by dropwise addition of biotinylated legs (15 nmol in 5 mL of HBS buffer, 3  $\mu\text{M}$ ) to ImmunoPure streptavidin (Pierce) (6 nmol in 10 mL of HBS buffer, 0.6  $\mu\text{M}$ ). The resulting crude solution was left at room temperature overnight. A slight excess of free biotin (1.2 equiv relative to the remaining free streptavidin binding sites), dissolved in 1 mL of HBS at pH 8, was added, and the solution was refrigerated at 4 °C for 15 min. The volume was reduced to ca. 1 mL by centrifugation through a membrane with a 30 kD molecular weight cutoff, at 5 °C. Assemblies with 1, 2, 3, and 4 catalytic units were isolated from the statistical mixture of products by IE HPLC, based on the procedure of Mirkin and colleagues but omitting EDTA.<sup>29</sup>

Assemblies with two streptavidins and six catalysts were synthesized by combining 2 equiv of assemblies with three catalysts (synthesized as described above, minus the addition of free D-biotin) with a 0.5 equiv of a bisbiotinylated linker. Final purification was again performed by IE HPLC. The yield for the total synthesis of six-unit assemblies is 1–2%.

All assemblies had IEC traces, UV spectra (260:280 nm ratios), and PAGE gels consistent with proposed structures and were at least 90% pure by IEC. Concentrations of the assemblies in solution were determined spectrophotometrically by absorbance at 260 nm via standard concentration curves. All species are stable in solution at +4 °C for prolonged periods of time.

We were unable to use mass spectrometry to obtain mass spectra of these noncovalent adducts (cf. other noncovalent adducts of this type<sup>29,32–35</sup>). Also, while HPLC gel filtration experiments showed a progressively increasing mass for species with 1–6 catalytic units, these masses could not be compared with a standard protein ladder because of the nonglobular nature of the species. Thus, we additionally confirmed the identity of individual assemblies with 1–4 legs by

(34) Eckart, K.; Spiess, J. *J. Am. Soc. Mass Spectrom.* **1995**, *6*(10), 912–9.

(35) Schwartz, B. L.; Gale, D. C.; Smith, R. D.; Chilkoti, A.; Stayton, P. S. *J. Mass Spectrom.* **1995**, *30*(8), 1095–102.

titration experiments with free legs, which would give only species with an increased number of legs (Supporting Information). A similar titration with linkers was performed with six-legged species. Furthermore, extensive degradation upon heating with excess D-biotin of six-legged species gave peaks identical in IE HPLC to the linker and legs.

**Preparation of Matrix-Displaying Substrates.** A 20  $\mu\text{M}$  solution of cleavable substrates (in HBS-EP) was applied to both channels of the SA sensor chip for 16 min at 5  $\mu\text{L min}^{-1}$ , followed by a 60 s wash with 4 M urea and 15 mM EDTA in both channels to remove any nonspecifically adsorbed material.

According to the Biacore SA chip literature, the matrix is a highly irregular 3D dextran hydrogel recognition matrix with a height of approximately 100–200 nm and an uneven distribution of streptavidin (Figure 2). We coated the matrix with biotinylated substrates containing two 18-atom hexaethylene glycol spacers between the biotin and the oligonucleotide. On the basis of changes in SPR response, substrates were coated at maximum densities of 0.25–0.31 pmol  $\text{mm}^{-2}$ , leading to an estimated effective concentration of 2.5–3.1 mM and an estimated intersubstrate distance of <9 nm. The estimated maximum amount of product released (that is, all the substrate cleaved) from the matrix is approximately 700 RU (based on the equation:  $\text{RU}(\mathbf{P}_2) = M_w(\mathbf{P}_2)\text{RU}(\mathbf{S})/M_w(\mathbf{S})$ ). The channel with only substrate deposited acted as a blank for correction of system influence, substrate dissociation, and substrate cleavage not attributed to deoxyribozymes.

**Cleavage of Substrates by Polycatalytic Assemblies.** The assemblies (1.5–6.3 nM in HBS-EP) were dispensed only to channel 2 at 5  $\mu\text{L min}^{-1}$ , with channel 1 used as a “no assembly” control. The load of assembly was controlled by adjusting concentrations and the reaction times of assemblies in the loading solution was calculated according to:

$$\text{ratio}(\text{assembly}/\mathbf{S}) = M_w(\mathbf{S})\text{RU}(\text{assembly})/[M_w(\text{assembly})\text{RU}(\mathbf{S})]$$

Monitoring the cleavage of the substrate was initiated by switching to the HBS-Zn buffer with a Biacore X system Working Tools Wash. Product formation in real time was measured through the decrease in mass, again using the formula 1000 RU = 1 ng  $\text{mm}^{-2}$ . Rates of cleavage were determined from the approximately linear region of the product release curves. In Figure 3, we show rates determined in the 5–9 min of cleavage. The first 5 min were not included because of the instability of the reading due to buffer changes and the release of nonspecifically bound material. The average substrate turnover for each spider is obtained from the number of products released until no more significant cleavage was observed (e.g., 200 min in Figure 4), while processivity is defined as the percentage of products released from the total product available for release. In several experiments, instrumental instabilities

were observed as occasional spikes in sensorgrams during long-time monitoring. Such spikes were manually removed, a procedure that does not influence any of the values reported in this manuscript.

**Substrate Turnover by Parent Deoxyribozymes.** For the single-leg experiment (that is, legs without a streptavidin), the 20  $\mu\text{M}$  cleavable substrate solution (in HBS-EP) was applied to channel 2 for 16 min at 5  $\mu\text{L min}^{-1}$ , followed by 1 min desorption with 4 M urea containing 15 mM EDTA. Channel 1 was treated with noncleavable substrate in the same fashion. Solutions of deoxyribozymes in HBS-Zn buffer were applied through both channels in HBS-Zn buffer for 1 min at 20  $\mu\text{L min}^{-1}$ . Flowing of this buffer was continued, and the sensorgram recorded until no further decrease in signal was observed. This method had a large experimental error because we estimated the loaded amount of deoxyribozymes on channel 2 from the response of channel 1. However, it allowed us to estimate the turnover of individual legs more precisely than did the approach used for the assemblies

**Acknowledgment.** Generous support from the Searle Scholars Program (to M.N.S.) and NSF grants IIS-0324845 (ITR Medium), CHE-0533065 (Chemical Bonding Center), and CCF-0523317 (EMT program) is gratefully acknowledged. D.S. is supported by NSF CAREER grant 0238027. We thank Paul Krapivsky for his advice on theoretical issues and a preprint of his paper (ref 20), Nils Walter and his students for their careful reading and comments on our manuscript (all mistakes and omissions are ours), Erik Winfree for inspiring discussions, and Don Landry for his support and encouragement.

**Supporting Information Available:** The following material is available: (1) IE and gel filtration HPLC conditions and profiles for the polycatalytic assemblies, including titration and demonstration experiments to demonstrate the number of legs; (2) fluorogenic cleavage by individual legs in solution (kinetic parameters);<sup>36,37</sup> (3) determination of  $k_{\text{on}}$  and  $k_{\text{off}}$  for  $\mathbf{P}_1$ -binding to its complements;<sup>38</sup> (4) binding of assemblies and single legs to product- and substrate-covered matrices. (5) Sensorgrams of spiders not shown in the manuscript. This material is available free of charge via the Internet at <http://pubs.acs.org>.

JA058394N

(36) Jenne, A.; Gmelin, W.; Raffler, N.; Famulok, M. *Angew. Chem., Int. Ed.* **1999**, *38*, 1300–3.

(37) Singh, K.; Parwaresch, R.; Krupp, G. *RNA* **1999**, *5*, 1348–56.

(38) Perkins, T. A.; Goodchild, J. *Methods Mol. Biol.* **1997**, *74*, *Ribozyyme Protocols*; Turner, P. C., Ed.; Humana Press, Inc.: Totowa, NJ; pp 241–52.